Desalination and Water Treatment
www.deswater.com

doi: 10.1080/19443994.2013.792161

51 (2013) 7523–7535
December

Taylor & Francis
Taylor & Francis Group

Removal of astrazon red 6B from aqueous solution using waste tea and spent tea bag

Emine Elmaslar Özbaş*, Atakan Öngen, Cemal Emre Gökçe

Faculty of Engineering, Department of Environmental Engineering, Istanbul University, Avcilar, Istanbul 34320, Turkey
Tel. +90 2124737070; Fax: +90 2124737180; email: elmaslar@istanbul.edu.tr

Received 29 March 2012; Accepted 6 March 2013

ABSTRACT

This study aimed to remove basic dye (astrazon red 6B (AR)) from liquid environment by adsorption. For this purpose, batch experiments were performed using spent tea leaves (TL) and tea bags (TB) as adsorbents due to their low costs. Adsorption experiments were carried out for different initial concentrations (25–200 mg/L), different pH values (pH 2–10), and different adsorbent amounts (0.25–2 g/L) of solution. Equilibrium sorption isotherms and kinetics were investigated. The experimental data were analyzed by the Langmuir, Freundlich and Temkin models of adsorption. The adsorption data fitted well to the Freundlich isotherm for TL and Langmuir isotherm for TB. Two kinetic models, pseudo-first order and pseudo-second order, were employed to describe the adsorption mechanism. According to the results of the analysis, the pseudo-second-order equation was determined to be the best model to describe the adsorption behavior for both adsorbents with the determination factor $R^2 \geqslant 0.92$. The results proved that the spent TL and used TB could be potentially used as low-cost adsorbents for the removal of AR from aqueous solutions.

Keywords: Adsorption; Astrazon red; Isotherm; Kinetics; Tea bag; Tea leaf

1. Introduction

Cationic dyes were commonly used initially for dying of silk, leather, plastics, paper, cotton mordanted with tannin and also in manufacturing of paints and printing inks [1,2]. Color produced by minute amount of organic dyes in water is considered very important for industrial water pollution due to its harmful effects and esthetically unpleasant appearance. Colored water can affect plant life and thus an entire ecosystem can be destroyed by the contamination of various dyes in water. Some dyes are also toxic and even carcinogenic. This dictates the necessity of dye containing water to undergo treatment before disposal to environment. Various conventional methods including biological and physical–chemical processes were used to remove color from wastewater [2–4]. These processes include solar photo-Fenton degradation [5], photocatalytic degradation [6], photo-Fenton processes [7], biodegradation [8], integrated chemical–biological degradation [9], electrochemical degradation [10], and adsorption [11].

However, these processes are not always effective and economic if solute concentrations are very low. Moreover, most of the synthetic organic dyes undergo very slow biodegradation. The adsorption technique

*Corresponding author.

appears to offer the best prospect over others and proves itself as one of the effective and attractive processes for the treatment of dye containing wastewater [12]. Moreover, this method becomes economically attractive and does not require any expensive additional pretreatment [2,13–16].

In fact, activated carbon (AC) is known to be a very effective adsorbent material due to its highly developed porosity, large surface area (that can reach 3,000 m^2/g), variable characteristic surface chemistry, and high degree of surface reactivity [17,18]. These unique characteristics make the AC a very versatile material that can remove a wide range of pollutants from various matrices. In addition, it has high adsorption capacity and fast adsorption kinetics [19]. However, its usage is limited due to the expensiveness increased with higher quality [17]. In recent years, attention has shifted toward the materials, which were by-products of wastes from large-scale industrial operations and agricultural waste materials. Major advantages of these materials are low cost, high efficiency, minimization of chemical or biological sludge, no additional nutrient requirement, and regeneration of adsorbent and possibility of effluent recovery [20]. In this regard, studies have been carried out to investigate various agricultural waste materials such as grass waste [21], rice hull [22], and cotton plant waste [23].

In recent years, a number of studies have been performed to develop alternative and economic adsorbents including palm ash [24], chitosan/oil palm ash composite beads [25], sodium montmorillonite clay [26], salts-treated beech sawdust [27], chitosan bead [28], biomass fly ash [29], zeolite [30], and almond shells [31].

Tea is basically the dried and processed leaves of only one species of plant called *Camellia sinensis* [32]. It is consumed by a large number of people in the world and considered the second most popular beverage in the world. Only water is rated higher in world consumption than tea. It is estimated that somewhere between 18 and 20 billion cups of tea are drunk daily on our planet. Canned or bottled tea as well as instant tea drinks is produced on an industrial scale by hot water extraction of tea leaves (TL), and the producers encounter the problem of disposing of the spent TL after the extraction. Hence, utilization of such waste is most desirable [21].

The objective of this study is to investigate the adsorption potential of spent TL and TB, abundantly available solid wastes, for the removal of astrazon red 6B (AR) from aqueous solution. The effects of various operating parameters such as solution pH, adsorbent dose, initial dye concentration, contact time on AR adsorption were investigated.

2. Materials and methods

2.1. Adsorbate

The basic dye used in this study was AR (C.I. Basic Red 46) (AR) purchased from Dystar, Turkey and used without further purification. The structure of AR is shown in Fig. 1.

2.2. Preparation of adsorbent

Spent black TB of the same brand were collected. Subsequently, the spent TL were removed from the TB and both were rinsed several times with boiled distilled water until the filtered water was cleared. Then, they were oven dried at 50°C for 48 h. Dried samples were ground and sieved to obtain particle sizes range of <2 mm for TL and 2–5 mm for tea bag. No other chemical or physical treatment was used prior to adsorption experiments.

2.2.1. Adsorbent characteristics

For SEM (scanning electron microscope) analysis, JEOL/JSM-6335F model scanning electron microscope with 370× and 400× magnification was used. The specific surface areas (BET) of adsorbents were derived from N_2 adsorption isotherms measured at liquid nitrogen temperature using Quantachrome Instruments Nova 4000E. These analyses were carried out at the Material Institute of the Scientific and Technological Research Council of Turkey (TÜBİTAK).

The infrared spectra of samples were obtained with Digilab, Exalibur-FTS 3000 MX model (USA) in the range of 400–4,000 cm^{-1} in the Advanced Analysis Laboratory (IAL) of Istanbul University. In order to prepare the sample pellets, samples were diluted with IR grade Merck KBr (samples/KBr: 1/200 (w/w)).

Percentages of C, H, N, and S in compost samples were determined at the IAL of Istanbul University. Prior to the elemental analysis, samples were dried at 50°C for 24 h and ground to a fine powder in a quartz mortar.

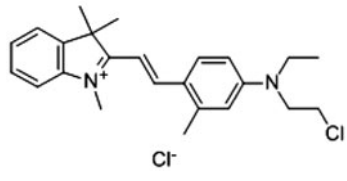

Fig. 1. Chemical structure of astrazon red 6B.

2.4. Effect of adsorbent dose

The effect of adsorbent doses on the amount of AR adsorbed was investigated by adding different amounts (0.25, 0.5, 1, 1.5, and 2 g/L) of TL and TB in 50 mg/L of dye solution. The pH of the solution was adjusted (pH 10 for TL and pH 9 for TB) with 0.1 M NaOH solution using a pH meter (Hanna Instruments pH213 pH meter) equipped with a combined electrode. Adsorption experiments were conducted in a thermostatic shaker bath at 25°C. The agitation was provided at 150 rpm for 240 min.

2.5. Equilibrium studies

Adsorption experiments were carried out by adding a fixed amount of adsorbent (0.5 g/L) into a number of 250-mL stoppered glass Erlenmeyer flasks containing a definite volume (200 mL in each flask) of different initial concentrations (25–200 mg/L) of dye solutions at pH 9 for TL and pH 10 for TB at a temperature of 25°C. The flasks were placed in a thermostatic shaker bath, and agitation was provided at 150 rpm for 240 min. The dye concentrations were measured at different times (0–240 min) with a 1.0 cm light path quartz cells using a spectrophotometer (Shimadzu UV1201) at λ_{max} of 525 nm. The amount of the adsorbed dye was calculated from the concentrations in the solution before and after the adsorption. The calibration curve was plotted from the dye solutions prepared in the concentration range of 2–300 mg/L. All experiments were run at least twice.

2.6. Effect of solution pH

In the study, 200 mL of dye solution of 50 mg/L initial concentration at different pH values (2–10) was agitated with 0.1 g of TL and TB in a thermostatic shaker bath at 25°C. Agitation was performed for 240 min at a constant agitation speed of 150 rpm. The dye concentrations were measured by a spectrophotometer. The pH values were adjusted with 0.1 M NaOH solution using a pH meter.

2.7. Batch kinetic studies

Several kinetic models are available to understand the behavior of the adsorbent, to examine the controlling mechanism of the adsorption process, and to test the experimental data. In the present study, the adsorption data were analyzed using two kinetic models: the pseudo-first-order and pseudo-second-order kinetic models. The conformity between the experimental data and the model-predicted values was expressed by the determination factor (R^2). A relatively high R^2 value indicates that the model successfully describes the kinetics of the dye adsorption. The pseudo-first-order model was introduced by Lagergren [33–35].

A pseudo-first-order equation can be expressed in a linear form (Eq. (1)):

$$\log(q_e - q_t) = \log(q_e) - (k_1/2.303)t \quad (1)$$

where q_e and q are the amounts of dye adsorbed (mg/g) on the adsorbents at the equilibrium and at time t, respectively, and k_1 is the rate constant of adsorption (min^{-1}). Values of k_1 were calculated from the plots of $\log(q_e–q_t)$ versus t for different concentrations of the basic dye.

The sorption data were also analyzed in terms of pseudo-second-order mechanism described in Refs. [33,34,36,37]:

The pseudo-second-order adsorption kinetic rate equation is expressed as follows (Eq. (2)):

$$dq_t/dt = k_2(q_e - q_t)^2 \quad (2)$$

Here, k_2 is the rate constant of pseudo-second-order adsorption (g/mg min). Integrating and applying the initial conditions, the equation can be presented as linear form (Eq. (3)):

$$t/q_t = [1/(k_2 q_e^2) + (1/q_e)(t) \quad (3)$$

Here, q_e is the amount of dye adsorbed at equilibrium (mg/g). The second-order rate constants were used to calculate the initial sorption rate, $h = k_2 q_e^2$ .Values of k_2 and q_e were calculated from the intercept and the slope of the linear plots of t/q_t versus t.

2.8. Adsorption isotherms

The adsorption isotherm indicates how the adsorbate molecules distribute between the liquid phase and the solid phase when the adsorption process reaches an equilibrium state. The analysis of the isotherm data by fitting them to different isotherm models is also an important step which can be used for design purposes [38,39]. Langmuir and Freundlich equations are commonly used in the adsorption isotherm studies. The Langmuir theory assumes that sorption takes place at specific sites within the adsorbent, which means that no further adsorption can take place at a site occupied by a dye molecule. Therefore, a saturation point is reached at equilibrium beyond which no further adsorption can occur, and the saturation monolayer can be then represented by the following expression (Eq. (4)) [40]:

$$(C_e/q_e) = (1/q_m K) + (1/q_m)C_e \quad (4)$$

where q_m is the maximum amount of adsorption (mg/g), K is the affinity constant (L/g), and C_e is the solution concentration at equilibrium (mg/L). The Freundlich model assumes that the sorption takes place on heterogeneous surfaces and adsorption capacity depends on the concentration of dyes at equilibrium. The well-known logarithmic form of Freundlich model is given by the following equation (Eq. (5)) [40]:

$$\ln q_e = \ln K_F + (1/n)\ln C_e \quad (5)$$

where K_F and n are the Freundlich constants related to the adsorption capacity and adsorption intensity, respectively. So, the plot of $\ln q_e$ against $\ln C_e$ of Eq. (5) should give a linear relationship whereby $1/n$ and K_F can be determined from the slope and the intercept, respectively.

The Temkin isotherm equation assumes that the heat of adsorption of all the molecules in layer decreases linearly with coverage due to adsorbent–adsorbate interactions, and that the adsorption is characterized by a uniform distribution of the bonding energies, up to some maximum binding energy [41].

The Temkin isotherm is given as:

$$\ln q_e = B \ln A + B \ln C_e \quad (6)$$

where A (l/g) is the equilibrium binding constant, corresponding to the maximum binding energy, and constant B is related to the heat of adsorption. A plot of q_e versus $\ln C_e$ enables the determination of the isotherm constants B and A from the slope and intercept of the straight line plot. The constant B is related to the heat of adsorption.

2.9. Analytical methods

The dye concentrations were monitored by measuring absorbance at 525 nm using a spectrophotometer (Shimadzu UV1201). The calibration curve was plotted from the dye solutions prepared in the concentration range of 2–300 mg/L.

3. Results and discussion

3.1. Adsorbent characteristics

Characteristics of the investigated adsorbents are presented in Table 1. SEM photographs are shown in Figs. 2 and 3.

Fig. 2 shows the SEM micrographs of tea leaf samples before and after the dye adsorption. Fig. 2(a) shows the rough surface morphology of TL with pores of different sizes. These pores are useful for dye adsorption. Fig. 2(b) shows the surface of dye-loaded adsorbent TL. As shown in Fig. 3(a) and (b), fibers of TB samples were swollen after the dye adsorption.

Table 1
Some characteristics of adsorbents used in the experiments

	Tea leaf	Tea bag
C (%)	41.12	53.66
H (%)	7.31	9.18
N (%)	3.45	0.25
BET surface area (m^2/g)	0.222	

3.2. Effect of adsorbent dose on dye adsorption

The effect of dosage on the adsorption of AR onto TL is illustrated in Fig. 4. At equilibrium time, the percent removal increased from 57 to 94% in response to an increase in TL dose from 0.25 to 2 g. The removal of AR increased basically due to the number of active sites and the increase in available surface area with dosage. The optimum dose was found to be 0.10 g of TL for 200 mL of AR solution.

Fig. 5 shows the effect of adsorbent dosage (TB) on the removal of AR. The percentage removal of AR increased with adsorbent dosage (from 40 to 89%). This can be attributed to the extended adsorbent surface area and availability of more adsorption sites resulting from the increasing dosage of the adsorbent.

3.3. Effect of solution pH on dye adsorption

Fig. 6 shows the effect of pH on the adsorption of AR onto TL, and Fig. 7 shows the effect of pH on the adsorption of AR onto TB. The experiments were conducted at 50 mg/L initial AR concentration, 0.50 g/L TL and TB doses and 25°C. pH was observed to have a significant influence on the adsorption process. AR is a cationic dye and exists in aqueous solution in the form of positively charged ions. As a charged species, the degree of its adsorption onto the adsorbent surface is primarily influenced by adsorbent's surface charge, which in turn is influenced by the solution pH. As shown in Fig. 6, the equilibrium adsorption capacity was minimum at pH 2 (44 mg/g) and increased up to 10 and then remained nearly constant (97.5 mg/g) over the initial pH 10 for AR adsorption onto TL. Similarly, as shown in Fig. 7, the equilibrium adsorption capacity was minimum at pH 2 (7.2 mg/g) and increased up to nine and then remained nearly constant (70.5 mg/g) over the initial pH 9 for AR

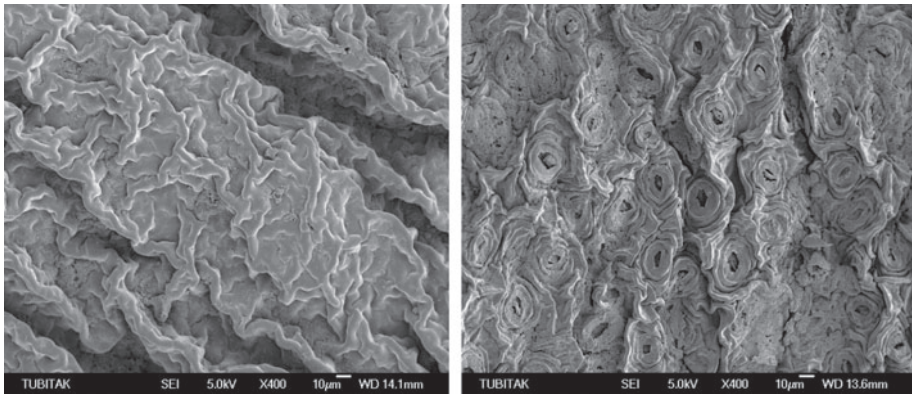

Fig. 2. SEM photographs of tea leaf before the dye sorption (a) and tea leaf with dye adsorbed (b).

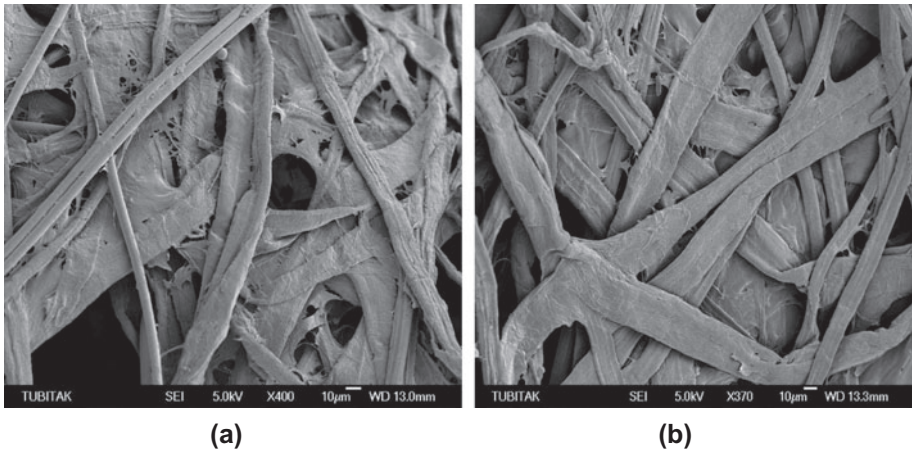

Fig. 3. SEM photographs of tea bag before the dye sorption (a) and tea bag with dye adsorbed (b).

adsorption onto TB. This phenomenon occurred due to the presence of excess H^+ ions in the adsorbate and the negatively charged surface adsorbent. Lower adsorption of AR at acidic pH is due to the presence of excess H^+ ions competing with the cation groups on the dye for adsorption sites. At higher levels of solution pH, the TL and TB possibly negatively charged and enhance the positively charged dye cations through electrostatic attraction force. A similar result was reported for the adsorption of AR onto the tea leaf [2].

3.4. Effect of contact time and initial concentration on dye adsorption

Figs. 8 and 9 show the effect of the initial dye concentration (50–500 mg/L) on the adsorption of AR. It was observed that AR was rapidly adsorbed by TL for the first 90 min, and thereafter, it proceeded at a slower rate and finally reached saturation (Fig. 8). On the other hand, AR was adsorbed onto TB for the first 45 min (Fig. 9). For AR adsorption onto TL, the equilibrium adsorption increased from 38 to 186 mg/g in parallel with an increase in the initial AR concentration from 25 to 200 mg/L. It was also found that the equilibrium removal of AR decreased from 75 to 46% as the initial AR concentration increased from 25 to 200 mg/L. For AR adsorption onto TB, the equilibrium adsorption increased from 33.14 to 105.6 mg/g in parallel with an increase in the initial AR concentration from 25 to 200 mg/L. In addition, the equilibrium removal of AR decreased from 66 to 26.4% as the initial AR concentration increased from 25 to 200 mg/L. These results could be attributed to the fact that the mass transfer driving force becomes larger and hence resulting in higher AR adsorption as the initial concentration increases. It is also shown in Figs 8 and 9 that the contact times needed for AR solutions with

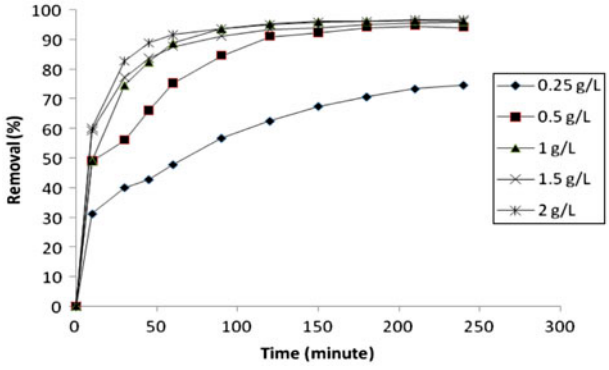

Fig. 4. Effect of adsorbent dosage on the adsorption of AR on TL (temperature = 25°C, C_0 = 50 mg/L, stirring rate = 150 rpm, pH = 10).

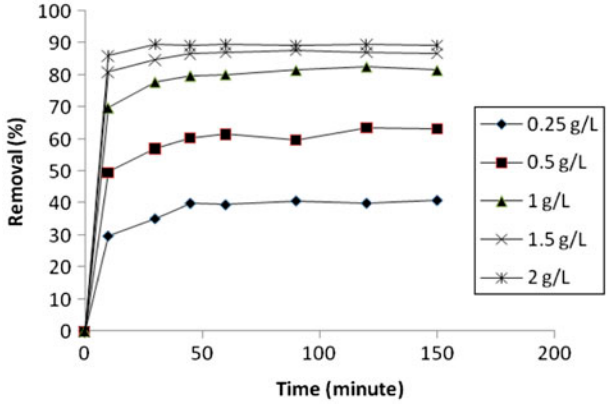

Fig. 5. Effect of adsorbent dosage on the adsorption of AR on TB (temperature = 25°C, C_0 = 50 mg/L, stirring rate = 150 rpm, pH = 9).

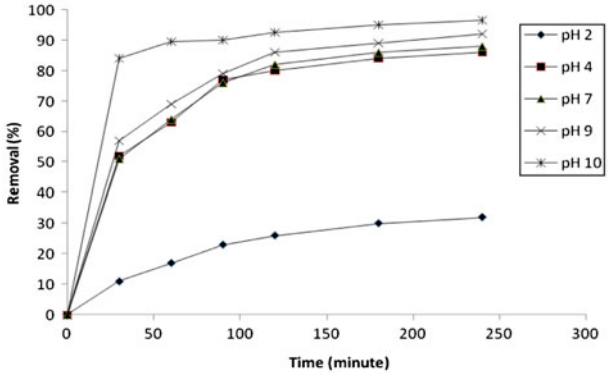

Fig. 6. Effect of pH on the adsorption of AR on TL (temperature = 25°C, C_0 = 50 mg/L, stirring rate = 150 rpm, 0.1 g/200 mL adsorbent).

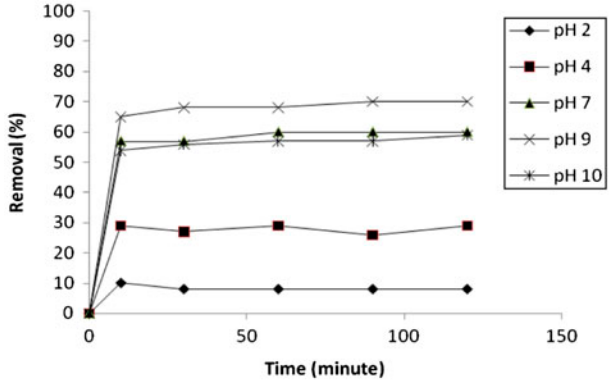

Fig. 7. Effect of pH on the adsorption of AR on TB (temperature = 25°C, C_0 = 50 mg/L, stirring rate = 150 rpm, 0.1 g/200 mL adsorbent).

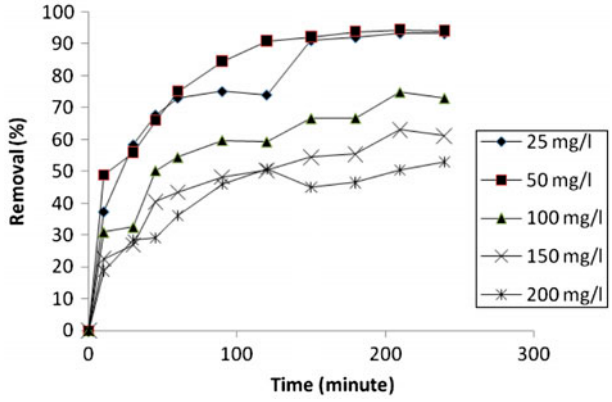

Fig. 8. Effect of contact time and initial concentration on the adsorption of AR on TL (temperature = 25°C, stirring rate = 150 rpm, 0.1 g/200 mL adsorbent, pH = 10).

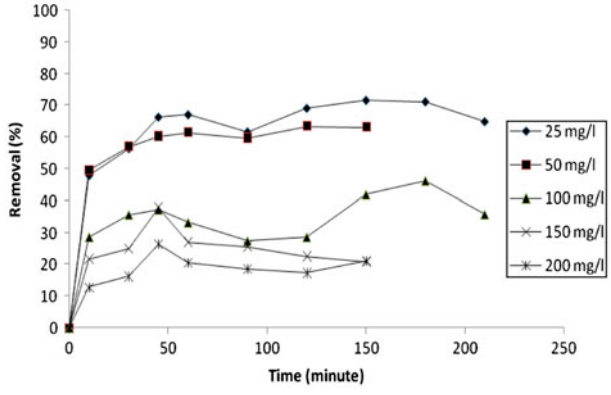

Fig. 9. Effect of contact time and initial concentration on the adsorption of AR on TB (temperature = 25°C, stirring rate = 150 rpm, 0.1 g/200 mL adsorbent, pH = 9).

initial concentrations of 25–200 mg/L to reach equilibrium were 90 and 45 min for adsorption on TL and TB, respectively. The initial concentration provides an important driving force to overcome all mass transfer resistances of AR between the aqueous and solid phase. However, the experimental data were measured at 240 min to be sure that full equilibrium was attained.

In the study, the optimum adsorbent dosage was determined for both tea TL and TB as 0.5 g/L. Assuming that a typical textile dye effluent stream has 500 m^3/day flow-rate, 250 kg adsorbent (tea leaf and tea bag) material would be required per day to clean the stream.

3.5. Adsorption kinetics

The transient behavior of the dye adsorption process was analyzed using the pseudo-first and pseudo-second-order kinetic models. The rate constants (k_1) evaluated from these plots (Figs. 10–13) with the obtained correlation coefficients are listed in Tables 2 and 3. The R^2 values listed for the pseudo-first-order kinetic model were between 0.5 and 0.99 (Tables 2 and 3), and 0.013 and 0.39 (Tables 2 and 3) for TL and TB, respectively. The R^2 values for pseudo-second-order model were between 0.93 and 0.999 (Tables 2 and 3), and 0.92 and 0.999 (Table 3) for TL and TB, respectively, which are higher than the obtained R^2 values for the pseudo-first-order model and closer to the unity. Therefore, the adsorption kinetics could be satisfactorily described by pseudo-second-order kinetic model for AR adsorption onto TL and TB. Similar phenomena were observed in sorption of MB onto mansonia (*Mansonia altissima*) wood sawdust [42]. Therefore, the results proved that the kinetics of AR adsorption on TL and TB followed pseudo-second-

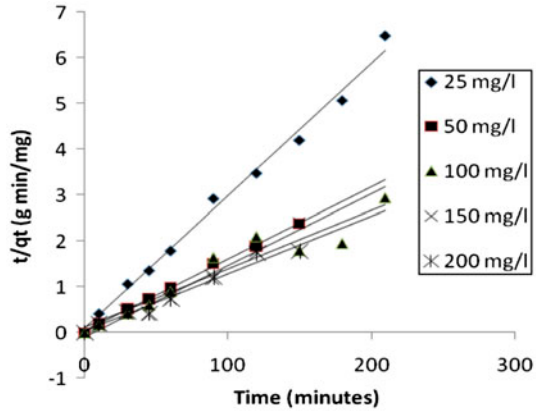

Fig. 11. The fitting of pseudo-second-order model for AR on TB for different initial concentrations (temperature = 25°C, stirring rate = 150 rpm, 0.1 g/200 mL adsorbent, pH = 10).

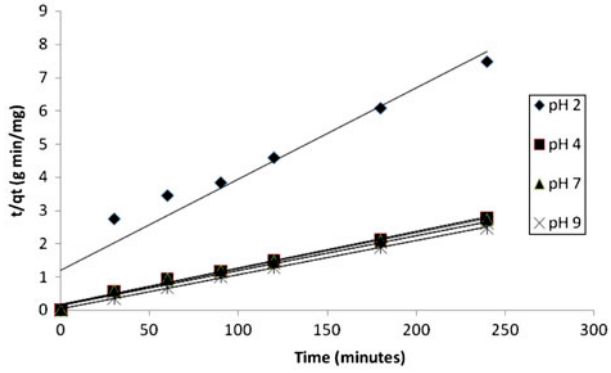

Fig. 12. The fitting of pseudo-second-order model for AR on TL for different pH values (temperature = 25°C, stirring rate = 150 rpm, 0.1 g/200 mL adsorbent, C_0 = 50 mg/L).

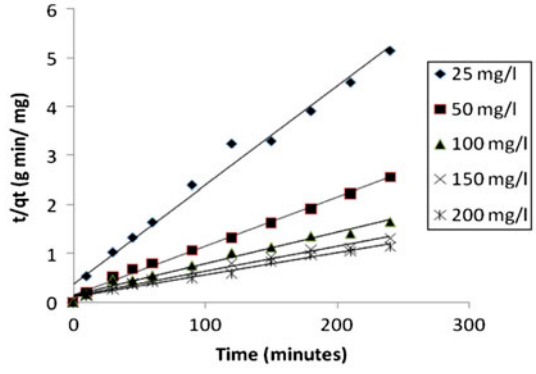

Fig. 10. The fitting of pseudo-second-order model for AR on TL for different initial concentrations (temperature = 25°C, stirring rate = 150 rpm, 0.1 g/200 mL adsorbent, pH = 9).

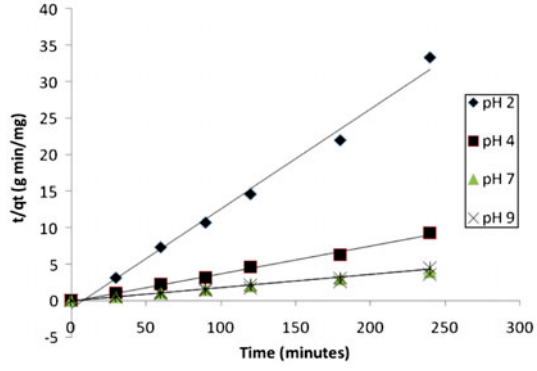

Fig. 13. The fitting of pseudo-second-order model for AR on TB for different pH values (temperature = 25°C, stirring rate = 150 rpm, 0.1 g/200 mL adsorbent, C_0 = 50 mg/L).

Table 2
Kinetics data calculated for adsorption of AR on TL

Parameters		Kinetic models							
C_0 (mg/L)	pH	Pseudo-first order		Pseudo-second order					
		R^2	k_1 (min^{-1})	$q_{e\ experimental}$ (mg/g)	$q_{e\ calculation}$ (mg/g)	R^2	k_2 (g/mg min)	$q_{e\ experimental}$ (mg/g)	$q_{e\ calculation}$ (mg/g)
25	10	0.76	0.0336238	46.76	76.86	0.99	0.0011	35.79	50
50	10	0.89	0.0343147	94.5	128.14	0.99	0.0007	63.36	100
100	10	0.51	0.0377692	149.73	382.12	0.98	0.0003	92.44	156
150	10	0.5	0.0382298	189.73	535.55	0.98	0.0002	113.79	200
200	10	0.76	0.0128968	212.17	143.52	0.98	0.0002	105.68	222
50	2	0.99	0.0057575	42.93	37.30	0.93	0.0006	42.93	36
50	4	0.98	0.0057575	94.39	41.16	0.99	0.0007	94.39	90
50	7	0.97	0.0057575	94.61	38.15	0.99	0.0006	94.61	93
50	9	0.96	0.0057575	96.17	33.53	0.99	0.0007	96.17	95
50	10	0.87	0.0052969	97.57	13.32	0.999	0.0025	97.57	97

Table 3
Kinetics data calculated for adsorption of AR on TB

Parameters		Kinetic models							
C_0 (mg/L)	pH	Pseudo-first order		Pseudo-second order					
		R^2	k_1 (min^{-1})	$q_{e\ experimental}$ (mg/g)	R^2	k_2	$q_{e\ calculation}$ (mg/g)	$q_{e\ experimental}$ (g/mg min)	$q_{e\ calculation}$ (mg/g)
25	9	0.39	0.002072	35.79	12.0	0.99	0.0097	35.79	34.6
50	9	0.7	0.043066	63.36	30.1	0.999	0.0065	63.36	63.7
100	9	0.5	0.031551	92.44	122.8	0.92	0.0014	92.44	78.7
150	9	5×10^{-3}	0.000460	113.79	13.7	0.98	0.0022	113.79	64.1
200	9	0.0013	0.002993	105.68	13.3	0.97	0.0086	105.68	79.4
50	2	0.1266	0.053429	9.6	14,444	0.99	0.0191	9.6	7.4
50	4	0.0023	0.001612	28.76	1.4	0.99	0.0156	28.76	26.5
50	7	0.3465	0.019114	60.23	4.8	0.999	0.0158	60.23	60.2
50	9	0.3257	0.018424	70.51	10.5	0.998	0.0212	70.51	68.0
50	10	0.2707	0.001611	58.87	10.4	0.99	0.0095	58.87	54.9

Table 4
Isotherm constants for AR on TL and TB

Adsorbent	Freundlich isotherm			Langmuir isotherm			Temkin ısotherm		
	K_F (mg/g)	n	R^2	q_m (mg/g)	K (L/g)	R^2	A (L/g)	B	R^2
Tea leaf	36	2.82	0.99	4.5×10^{-3}	3.76	0.89	3.082×10^{-6}	4.39	0.61
Tea bag	21	3.60	0.88	0.011	4.87	0.99	1.063×10^{-26}	0.31	0.0428

order model, suggesting that chemisorption might be the rate-limiting step that controlled the adsorption process.

3.6. Isotherm studies

In the present study, the equilibrium isotherms were analyzed using the Langmuir and Freundlich isotherms. The applicability of the isotherm models to the adsorption study was judged by the R^2 value of each plot. The higher the R^2 value, the better the fit. All the isotherm constants calculated by both models are listed in Table 4. It can be seen from the R^2 values, which are indicators of good-fit, that the Langmuir ($R^2 = 0.99$) exhibited better fit for adsorption of AR on TB compared to the Freundlich ($R^2 = 0.88$) and Temkin ($R^2 = 0.0428$) models (Table 4, Fig. 14). This could be caused by the homogeneous distribution of active sites onto TB surface [43,44]. It can be seen from Fig. 15 and Table 4 that Freundlich isotherm fits the data better than Langmuir and Temkin isotherms for adsorption of AR on TL. This is also confirmed by the high value of R^2 for Freundlich (0.99) compared to Langmuir (0.89) and Temkin (0.61). One of the Freundlich constants (K_F) demonstrated the adsorption capacity of the adsorbent. The other Freundlich constant (n) is a measure of the deviation from linearity of the adsorption. If n is equal to the unity, the adsorption is linear. However, if a value for n is below to the unity, adsorption process is concluded as chemical; on the other hand, n values above the unity indicate that adsorption is a favorable physical process [45–47]. The equilibrium value of n is 2.05, which represents the favorable adsorption, and suggests that physical adsorption is dominant rather than chemical adsorption when it is used for AR adsorption, which indicates weak adsorption bonds [42] and the presence of Van Der Waals forces.

3.7. IR characterization of adsorbents

The FTIR spectrum of astrozon red 6B is illustrated in Fig. 16. As seen from the figure, the FTIR spectrum displays all the characteristic IR peaks of consisting groups of the dye. In addition, the adsorption peaks and the assigned groups could be listed as (cm^{-1}): 2,926 and 2,854 (C–H stretching); 1,649 (C=C vibrations, non-conjugated); 1,605 and 1,545 (skeletal vibrations of aromatic ring); 1,456 and 1,400 (C–H); the region 1,340 (aromatic C–H and C–$(CH_3)_2$ vibrations); 1,258, 934, 862, and 835 (1, 2-di and 1, 2, 4-tri substituted aromatic ring vibrations); 1,128 (C–N vibrations) and 617 (C–Cl vibrations) [48,49]. Fig. 16 also

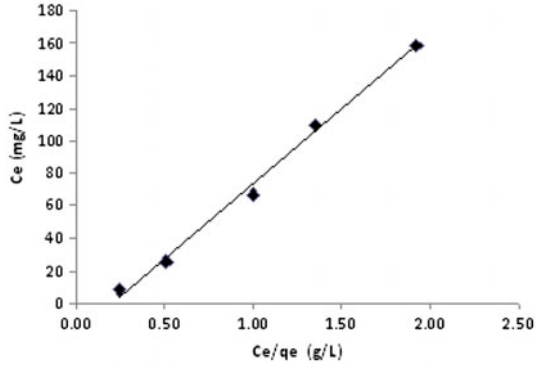

Fig. 14. Langmuir isotherm for the adsorption of AR onto TB (temperature = 25°C, stirring rate = 150 rpm, 0.1 g/200 mL adsorbent, $C_0 = 50$ mg/L).

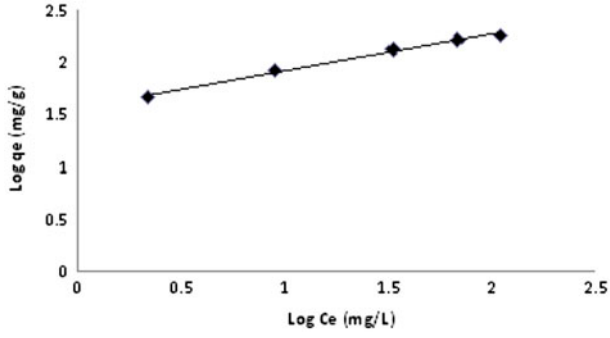

Fig. 15. Freundlich isotherm for adsorption of AR onto TL (temperature = 25°C, stirring rate = 150 rpm, 0.1 g/200 mL adsorbent, $C_0 = 50$ mg/L).

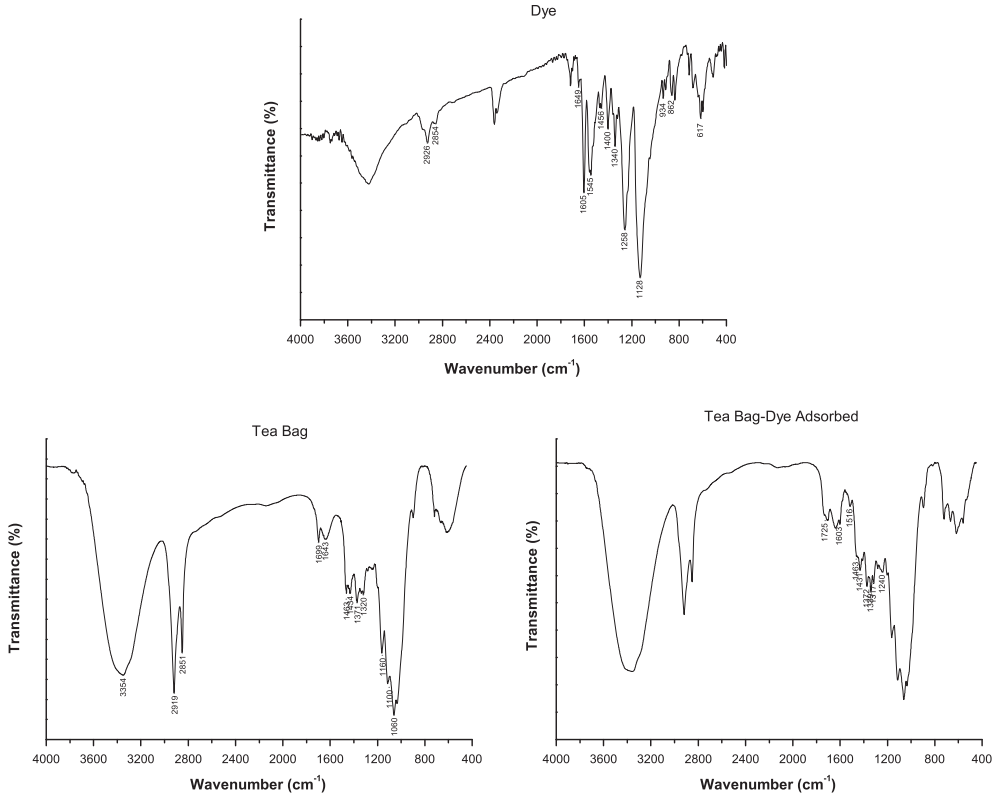

Fig. 16. FTIR spectrums of dye, tea bag and tea bag after the adsorption.

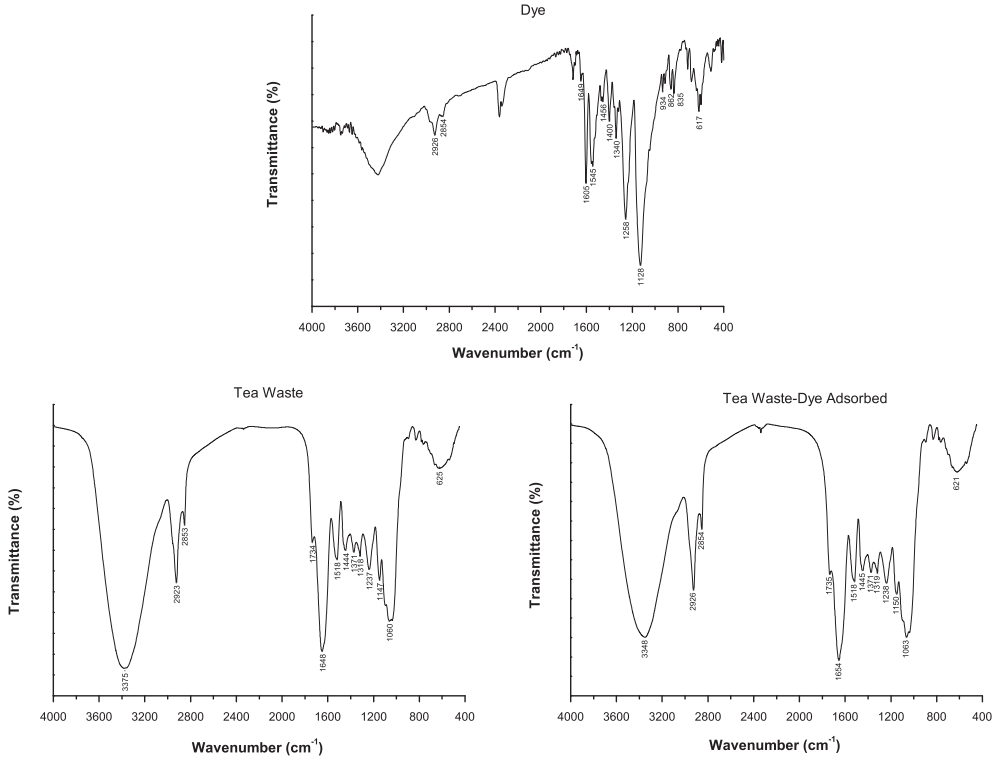

Fig. 17. FTIR spectrums of dye, tea leaf and tea leaf after the adsorption.

illustrates the FTIR spectrum of tea bag. As is well known, the TB is a cellulose-based material and the spectrum shows all the characteristic IR peaks of cellulose listed as (cm^{-1}): 3,354 (OH vibrations); 2,919 and 2,851 (C–H vibrations due to methyl and methylene groups); 1,699 (C=O vibration); 1,643 (C=C); 1,371 (CH_2OH vibrations); 1,463 and 1,433 (oxymethyl group vibrations); and 1,060–1,164 (region of C–O groups) [48,49]. Some differences were observed in the adsorption peaks of FTIR spectrum of TB following the dye adsorption. New peak values were observed due to the characteristic peaks of AR due to its adsorption on to tea bag surface; that is, a shoulder at 1,725 cm^{-1}, peaks at 1,603, 1,516, 1,240 cm^{-1}, etc. And, the intensity of the peaks at 1,317 and 1,339 cm^{-1} was increased due to the interaction of the same adsorption bands of AR. In addition, some intensity changes were also observed, that is: at 1,463 and 1,372 cm^{-1} which implied that the –OH groups of AR were the main adsorption points in this process.

The FTIR spectra before and after the adsorption of tea leaf are shown in Fig. 17, and the characteristic FTIR bands of the related groups are shown in Table 5. As shown in Fig. 17, the spectrum of TL displays a number of absorption peaks, indicating its complex nature. In the spectrum of TL, the broad band around 3,375 cm^{-1} represents the bonded –OH groups; on the other hand, the bands observed around 2,923 and 2,853 cm^{-1} were assigned to the aliphatic C–H groups. The peaks around 1,734 and 1,648 cm^{-1} correspond to the C=O stretching of carboxyl groups and amide groups (amide I band), respectively. The peak observed at 1,518 cm^{-1} was caused by amide II band which was attributed to the bending of N–H bonds, and the peak around 1,318 cm^{-1} was attributed to C–N stretching, amide III band. Symmetric bending of CH_3 groups was observed at 1,444 and 1,371 cm^{-1}; in addition, the characteristic peaks of $–SO_3$ groups due to asymmetric and symmetric stretching of $–SO_3$ groups were observed at 1,237 and 1,060, respectively. Finally, the peaks at 1,147 and 625 cm^{-1} could be assigned to C–O stretching of ether groups and –CN stretching, respectively [48,49]. As illustrated in Fig. 17, the dye and TL had similar adsorption peaks at their FTIR spectra. Thus, the adsorption process could not be identified by the observation of new IR peaks after the adsorption. But, as seen in Table 5, the spectral analysis before and after the dye adsorption indicated clear band shifts and lower intensity of the IR bands of –OH, SO_3, amide, and ether groups. These results demonstrated that the bioadsorption of the dye occurred during the interactions between the dye and so-called groups.

Table 5
IR characteristics of tea waste before and after the adsorption

Frequency (cm^{-1})			
Before adsorption	After adsorption	Differences	Assignment
3,375	3,348	−27	Bonded –OH
2,923	2,926	+3	Aliphatic C–H
2,853	2,854	+1	Aliphatic C–H
1,734	1,735	+1	C=O (carboxyl)
1,648	1,654	+6	Amide I
1,518	1,518	0	Amide II
1,444	1,445	+1	$–CH_3$
1,371	1,371	0	$–CH_3$
1,318	1,319	+1	Amide III
1,237	1,238	+1	$–SO_3$
1,147	1,150	+3	C–O (ether)
1,060	1,063	+3	$–SO_3$
625	621	−4	–CN

4. Conclusions

TL and TB were proven to be effective low-cost adsorbents for the removal of AR from aqueous solution via adsorption. The equilibrium data were analyzed using the Langmuir, Freundlich, and Temkin isotherm models. The adsorption equilibrium of AR onto TB was best described by the Langmuir isotherm model, while the adsorption equilibrium of AR onto TL was best described by the Freundlich isotherm model. Kinetics of the adsorption was also observed on TB and TL, and the processes were determined to continue via pseudo-second-order kinetics. Although TL and TB used for this work were not treated chemically or thermally, results showed that TL and TB have been good adsorbents and could be used as low-cost adsorbents for the removal of basic dye from solution. TL and TB are available in the tea factories and cafeterias. However, a suitable mechanism for collection and storing of TL and TB should be taken into account. Further investigations are needed for desorption studies, economically feasible regeneration of the adsorbent and application of the adsorbent for real industrial wastewater. However, in many countries of the world where waste TL and waste TB are available at low or no cost, maybe regeneration is not required and the used adsorbents can be disposed by incineration.

Abbreviations

A	—	the equilibrium binding constant (L/g),
AC	—	activated carbon
AR	—	astrazon red 6B
B	—	constant related to the heat of adsorption
BET	—	specific surface area (m^2/g)
C_0	—	initial concentration of dye (mg/L)
C_e	—	concentration of dye in solution after equilibrium (mg/L)
K	—	Langmuir affinity constant (L/g)
k_1	—	pseudo-first-order rate constant (min^{-1})
k_2	—	pseudo-second-order rate constant (g/mg min)
K_F and n	—	Freundlich constants related to adsorption capacity and adsorption intensity
q_e	—	experimental amounts of dye adsorbed at equilibrium time, (mg/g)
q_e	—	calculated amounts of dye adsorbed at equilibrium time (mg/g)
q_t	—	amounts of dye adsorbed at time t (mg/g)
q_m	—	amount of solute adsorbed per unit weight of adsorbent in forming a complete monolayer on the surface (mg/g)
R^2	—	determination factor
SEM	—	scanning electron microscope
t	—	time (minute)
TB	—	tea bag
TL	—	tea leaf

References

[1] H. Berneth, A.G. Bayer, Ullmann's Encyclopedia of Industrial Chemistry, Wiley-VCH Press, Weinheim, 2003.

[2] N. Nasuha, B.H. Hameed, A.T. Mohd Din, Rejected tea as a potential low-cost adsorbent for the removal of methylene blue, J. Hazard. Mater. 175 (2010) 126–132.

[3] K.V. Kumar, A. Kumaran, Removal of methylene blue by mango seed kernel powder, Biochem. Eng. J. 27 (2005) 83–93.

[4] V. Vadivelan, K.V. Kumar, Equilibrium, kinetics, mechanism, and process design for the sorption of methylene blue onto rice husk, J. Colloid Interface Sci. 286 (2005) 90–100.

[5] A. Duran, J.M. Monteagudo, E. Amores, Solar photo-Fenton degradation of reactive blue 4 in a CPC reactor, Appl. Catal. B 80 (2008) 42–50.

[6] J. Sun, L. Qiao, S. Sun, G. Wang, Photocatalytic degradation of Orange G on nitrogen-doped TiO_2 catalysts under visible light and sunlight irradiation, J. Hazard. Mater. 155 (2008) 312–319.

[7] w?>J. Garcia-Monta~no, N. Ruiz, I. Mu~noz, X. Domenech, J.A. Garcia-Hortal, F. Torrades, J. Peral, Environmental assessment of different photo-Fenton approaches for commercial reactive dye removal, J. Hazard. Mater. 138 (2006) 218–225.

[8] W. Azmi, R.K. Sani, U.C. Banerjee, Biodegradation of triphenylmethane dyes, Enzyme Microb. Technol. 22 (1998) 185–191.

[9] G. Sudarjanto, B. Keller-Lehmann, J. Keller, Optimization of integrated chemical biological degradation of a reactive azo dye using response surface methodology, J. Hazard. Mater. 138 (2006) 160–168.

[10] L. Fan, Y. Zhou, W. Yang, G. Chen, F. Yang, Electrochemical degradation of aqueous solution of Amaranth azo dye on ACF under potentiostatic model, Dyes Pigm. 76 (2008) 440–446.

[11] B.H. Hameed, A.A. Ahmad, Batch adsorption of methylene blue from aqueous solution by garlic peel, an agricultural waste biomass, J. Hazard. Mater. 164 (2009) 870–875.

[12] S. Wang, Y. Boyjoo, A. Choueib, Removal of dyes from aqueous solution using fly ash and red mud, Water Res. 39 (2005) 129–138.

[13] A.K. Jain, V.K. Gupta, A. Bhatnagar, A. Suhas, A comparative study of adsorbents prepared from industrial wastes for removal of dyes, Sep. Sci. Technol. 38 (2003) 463–481.

[14] T. Sauer, G. Cesconeto Neto, H.J. Jose, R.F.P.M. Mureira, Kinetics of photocatalytic degradation of reactive dyes in a TiO_2 slurry reactor, J. Photochem. Photobiol. A 149 (2002) 147–154.

[15] Md T. Uddin, Md A. Islam, S. Mahmud, Md. Rukanuzzaman, Adsorptive removal of methylene blue by tea waste, J. Hazard. Mater. 164 (2009) 53–60.

[16] G.M. Walker, L. Hansen, J.A. Hanna, S.J. Allen, Kinetics of reactive dye adsorption onto dolomitic sorbents, Water Res. 37 (2003) 2081–2089.

[17] R. Arriagada, R. Garcia, M. Molina-Sabio, F. Rodriguez-Reinoso, Effect of steam activation on the porosity and chemical nature of activated carbons from Eucalyptus globules and peach stones, Microporous Mater. 8 (1997) 123–130.

[18] R.C. Bansal, J.B. Donnet, H.F. Stoeckli, Active Carbon, Marcel Dekker, New York, NY, 7–11 1988.

[19] F.L. Slejko, Adsorption Technology: A Step by Step Approach to Process Evaluation Application, Marcel Dekker, New York, NY, 1985.

[20] D. Sud, G. Mahajan, M.P. Kaur, Agricultural waste material as potential adsorbent for sequestering heavy metal ions from aqueous solutions: A review, Bioresour. Technol. 99 (2008) 6017–6027.

[21] B.H. Hameed, Grass waste: A novel sorbent for the removal of basic dye from aqueous solution, J. Hazard. Mater. 166 (2009) 233–238.

[22] S.T. Ong, C.K. Lee, Z. Zainal, Removal of basic and reactive dyes using ethylenediamine modified rice hull, Bioresour. Technol. 98 (2007) 2792–2799.

[23] O. Tunç, H. Tanaci, Z. Aksu, Potential use of cotton plant wastes for the removal of Remazol Black B reactive dye, J. Hazard. Mater. 163 (2009) 187–198.

[24] A.A. Ahmad, B.H. Hameed, N. Aziz, Adsorption of direct dye on palm ash: Kinetic and equilibrium modeling, J. Hazard. Mater. 141 (2007) 70–76.

[25] M. Hasan, B.H. Hameed, A.L. Ahmad, Adsorption of reactive dye onto crosslinked chitosan/oil palm ash composite beads, Chem. Eng. J. 136 (2008) 164–172.

[26] P.P. Selvam, S. Preethi, P. Basakaralingam, N. Thinakaran, A. Sivasamy, S. Sivanesan, Removal of rhodamine B from-aqueous solution by adsorption onto sodium Montmorillonite, J. Hazard. Mater. 155 (2008) 39–44.

[27] F.A. Batzias, D.K. Sidiras, Simulation of methylene blue adsorption by salts-treated beech sawdust in batch and fixed-bed systems, J. Hazard. Mater. 149 (2007) 8–17.

[28] Z. Bekçi, C. Ozveri, Y. Seki, K. Yurdakoç, Sorption of malachite green on chitosan bead, J. Hazard. Mater. 154 (2008) 254–261.

[29] P. Pengthamkeerati, T. Satapanajaru, O. Singchan, Sorption of reactive dye from aqueous solution on biomass fly ash, J. Hazard. Mater. 153 (2008) 1149–1156.

[30] S.K. Alpat, O. Ozbayrak, Ş. Alpat, H. Akçay, The adsorption kinetics and removal of cationic dye Toluidine Blue O, from aqueous solution with Turkish zeolite, J. Hazard. Mater. 151 (2008) 213–220.

[31] F. Doulati Ardejani, K.H. Badii, N. Yousefi Limaee, S.Z. Shafaei, A.R. Mirhabibi, Adsorption of Direct Red 80 dye from aqueous solution onto almond shells: effect of pH, initial concentration and shell type, J. Hazard. Mater. 151 (2008) 730–737.
[32] N.S. Mokgalaka, R.I. McCrindle, B.M. Botha, Multielement analysis of tea leaves by inductively coupled plasma optical emission spectrometry using slurry nebulization, J. Anal. At. Spectrom. 19 (2004) 1375–1378.
[33] M.Ç. Akkaya, S. Emik, G. Güçlü, T.B. İyim, S. Özgümüş, Removal of basic dyes from aqueous solutions by cross-linked-acrylicacid/acrylamidopropane sulfonic acid hydrogels, J. Appl. Polym. Sci. 114 (2009) 1150–1159.
[34] M. Dalaran, S. Emik, G. Guclu, T.B. İyim, S. Özgümüş, Removal of acidic dye from aqueous solutions using poly (DMAEMA-AMPS-HEMA) terpolymer/MMT nano composite hydrogels, Polym. Bull. 63(2) (2009) 159–171.
[35] S. Lagergren, To the theory of the so-called gel adsorption, The Royal Swedish Academy of Sciences, Document 24 (1898) 1–39.
[36] M.I. El-Khaiary, Kinetics and mechanism of adsorption of methylene blue from aqueous solution by nitric-acid treated water-hyacinth, J. Hazard. Mater. 147 (2007) 28–36.
[37] A. Gürses, C. Doğar, M. Yalçın, M. Açıkyıldız, R. Bayrak, S. Karaca, The adsorption kinetics of the cationic dye methylene blue onto clay, J. Hazard. Mater. 131 (2006) 217–228.
[38] M. El-Guendi, Homogeneous surface diffusion model of basic dyestuffs onto natural clay in batch adsorbers, Adsorpt. Sci. Technol. 8 (1991) 217–225.
[39] Y. Özdemir, M. Doğan, M. Alkan, Adsorption of cationic dyes from aqueous solutions by sepiolite, Microporous Mesoporous Mater. 96 (2006) 419–427.
[40] E. Rubin, P. Rodriguez, R. Herrero, J. Cremades, I. Barbara, M.E. Sastre de Vicente, Removal of methylene blue from aqueous solutions using as biosorbent Sargassum muticum: An invasive macroalga in Europe, J. Chem. Technol. Biotechnol. 80 (2005) 291–298.
[41] M.J. Temkin, V. Pyzhev, Recent modifications to Langmuir Isotherms, Acta Phys. Chim. USSR 12 (1940) 217–222.
[42] A.E. Ofomaja, Kinetic study and sorption mechanism of methylene blue and methyl violet onto mansonia (*Mansonia altissima*) wood sawdust, Chem. Eng. J. 143 (2008) 85–95.
[43] M. Alkan, Ö. Demirbaş, S. Çelikçapa, M. Doğan, Sorption of acid red 57 from aqueous solution onto sepiolite, J. Hazard. Mater. 116 (2004) 135–145.
[44] C.A.P. Almeida, A. Dos Santos, S. Jaerger, N.A. Debacher, N.P. Hankins, Mineral waste from coal mining for removal of astrazon red dye from aqueous solutions, Desalination 264 (2010) 181–187.
[45] S.K. Behera, J.-H. Kim, X. Guo, H.-S. Park, Adsorption equilibrium and kinetics of polyvinyl alcohol from aqueous solution on powdered activated carbon, J. Hazard. Mater. 153(3) (2008) 1207–1214.
[46] P.P. Selvam, S. Preethi, P. Basakaralingam, N. Thinakaran, A. Sivasamy, S. Sivanesan, Removal of rhodamine B from aqueous solution by adsorption onto sodium montmorillonite, J. Hazard. Mater. 155(1–2) (2008) 9–44.
[47] M.-H. Baek, C.O. Ijagbemi, S.-J. O , D.-S. Kim, Removal of malachite green from aqueous solution using degreased coffee bean, J. Hazard. Mater. 176 (2010) 820–828.
[48] L.J. Bellamy, The Infra-Red Spectra of Complex Molecules, Chapman and Hall, London, 1975.
[49] N.V. Ivanova, E.A. Korolenko, E.V. Korolik, R.G. Zhbankov, IR spectrum of cellulose, Zh. Prikl. Spektrosk. 51 (1989) 301–306.